Coherent coupled-reaction-channels analysis of existing and new $p + {}^{9}$Be data between 1.7 and 15 MeV/nucleon

N. Keeley,[1,*] A. Pakou,[2,†] V. Soukeras,[2,3] F. Cappuzzello,[3,4] L. Acosta,[5,6] C. Agodi,[3] A. Boiano,[7] S. Calabrese,[3,4] D. Carbone,[3] M. Cavallaro,[3] N. Deshmukh,[3,‡] A. Foti,[4,6] A. Hacisalihoglu,[3] M. La Commara,[7,8] I. Martel,[9,§] M. Mazzocco,[10,11] A. Muoio,[3] C. Parascandolo,[7] D. Pierroutsakou,[7] K. Rusek,[12] A. M. Sanchez-Benitez,[13] G. Santagati,[3] O. Sgouros,[2,3] G. Souliotis,[14] A. Spatafora,[3,4] E. Strano,[10,11] D. Torresi,[3] and A. Trzcinska[12]

[1]*National Centre for Nuclear Research, ul. Andrzeja Sołtana 7, 05-400 Otwock, Poland*
[2]*Department of Physics and HINP, University of Ioannina, 45110 Ioannina, Greece*
[3]*INFN Laboratori Nazionali del Sud, Via S. Sofia 62, 95125 Catania, Italy*
[4]*Dipartimento di Fisica e Astronomia, Universita di Catania, Via S. Sofia 64, 95125 Catania, Italy*
[5]*Instituto de Fisica, Universidad Nacional Autonoma de Mexico, Mexico Distrito Federal 01000, Mexico*
[6]*INFN - Sezione di Catania, Via S. Sofia 64, 95125 Catania, Italy*
[7]*INFN - Sezione di Napoli, Via Cinthia, I-80126 Napoli, Italy*
[8]*Dipartimento di Scienze Fisiche, Università di Napoli "Federico II",via Cintia, I-80126 Napoli, Italy*
[9]*Department of Physics, University of Liverpool, Liverpool L69 7ZE, United Kingdom*
[10]*Departimento di Fisica e Astronomia, Universita di Padova, Via Marzolo 8, I-35131, Padova, Italy*
[11]*INFN - Sezione di Padova, Via Marzolo 8, I-35131, Padova, Italy*
[12]*Heavy Ion Laboratory, University of Warsaw, ul. Pasteura 5a, 02-093, Warsaw, Poland*
[13]*Centro de Estudios Avanzados en Física, Matemáticas y Computación (CEAFMC), Department of Integrated Sciences, University of Huelva, 21071 Huelva, Spain*
[14]*Department of Chemistry, National and Kapodistrian University of Athens and HINP, 15771 Athens, Greece*

(Received 10 December 2018; published 18 January 2019)

New data for the elastic scattering of ^{9}Be from protons were obtained and analyzed together with data from the literature in a coherent coupled-reaction-channels approach. The new measurements were performed in inverse kinematics at 15, 22 and 51 MeV (1.67, 2.44, and 5.67 MeV/nucleon) by detecting the heavy ejectile in the MAGNEX spectrometer. This enabled an almost full angular distribution to be obtained, extending the results to forward angles where calculated values coincide and give the opportunity of proper normalization. Previous inconsistencies in absolute normalization between different data sets are removed. Standard collective model form factors fail to reproduce the inelastic scattering to the 2.43 MeV $5/2^{-}$ state of ^{9}Be, suggesting that a more sophisticated approach based on the cluster structure of ^{9}Be is required to describe this process.

DOI: 10.1103/PhysRevC.99.014615

I. INTRODUCTION

Our ongoing systematic study of the interactions of protons with light weakly bound nuclei in inverse kinematics, completed for ^{6,7}Li with measurements of elastic scattering [1–3] and reactions [3–7], is here extended to the elastic scattering of the Borromean nucleus ^{9}Be. This nucleus still attracts considerable interest due to its role in astrophysical problems of building up the heavy elements and triggering the *r* process [8–11]. Furthermore, it is an excellent example of a nucleus that is best described by clustering theories [12].

There are several data sets in the literature covering both scattering and reactions for the $p + {}^{9}$Be system in the energy region of interest to this study. However, while most of these sets are internally consistent since they were measured in a single experiment with the same target and detection setup employed throughout, the absolute cross section normalizations can differ by 15–20% between different measurements. Therefore, within our experimental program one of the first tasks was to focus on a precise elastic scattering measurement in order to obtain an absolute normalization that was as accurate as possible. By means of a coherent theoretical analysis of the new and existing data, we aimed both to validate the normalization of the new data and arrive at a consistent composite data set covering a relatively large range of incident proton energies. The present work should thus provide a useful confirmation of the experimental setup for future measurements using MAGNEX with radioactive projectiles in inverse kinematics.

In the theoretical analysis we elected to take the elastic scattering data of Votava *et al.* [13] as our "benchmark," in particular their measurement of the elastic and inelastic scattering to the 2.43 MeV $5/2^{-}$ state of ^{9}Be at an incident

*nicholas.keeley@ncbj.gov.pl
†apakou@uoi.gr
‡Permanent address: Nuclear Physics Division, Saha Institute of Nuclear Physics, Kolkata-INDIA.
§On sabbatical from Department of Physics, University of Huelva, Spain.

proton energy of 15 MeV. This data set was chosen for a variety of reasons: at 15 MeV there is a rather complete data set for the elastic and inelastic scattering plus the (p, d) reaction (from a separate source [14]); it overlaps with the extensive elastic and inelastic scattering data set of Bingham *et al.* [15], thus enabling their relative normalizations to be fixed; and, finally, the normalization of this data set seems to be consistent with as many as possible of the other data sets at lower incident energies. However, we acknowledge that other data sets might have been taken as the benchmark with equal propriety. The renormalizations required to obtain an internally consistent data set are fully documented in Sec. III. The analysis proceeded in a coherent manner for these data down to the lower energies where the present precise elastic scattering measurements fit into the sequence. The absolute normalizations of the new data were found to be consistent with this coherent analysis, thus providing an important benchmark for future experiments using MAGNEX.

The structure of the paper is as follows: in Sec. II we give details of the experiment, in Sec. III we give an overview of existing data and their absolute normalizations, in Sec. IV the coupled-reaction-channels (CRC) analysis is described, and finally Sec. V provides a discussion with a summary of the results.

II. EXPERIMENTAL DETAILS

The experiment was performed at the MAGNEX facility of the Istituto Nazionale di Fisica Nucleare Laboratori Nazionali del Sud (INFN-LNS) in Catania, Italy. A $^{9}Be^{4+}$ beam was accelerated by the TANDEM Van de Graaff accelerator of LNS to 15, 22, and 51 MeV and impinged on 232 and 450 μg/cm^2 CH_2 targets at the lower and higher energies, respectively. The measurement was repeated with a 290 μg/cm^2 ^{12}C target to estimate any contamination due to the carbon included in the main targets.

The experiment was designed to employ inverse kinematics to access the heavy ejectile over almost the full angular range by holding the MAGNEX [16] spectrometer at one position but changing accordingly two to three magnetic fields. The spectrometer was operated with the optical axis set at $\theta_{\rm opt} = 7.7^\circ$, covering an angular range between 2.5° and 14° in the laboratory frame. The data reduction technique used with MAGNEX is based on the ray reconstruction of the data, and is described in Refs. [17–19]. A typical reconstructed energy-theta correlation plot for the highest energy proton scattering is presented in Fig. 1. Data for the first and second solutions are designated by different colors (red for the first and blue for the second solution) and were obtained by applying two different magnetic fields. In the same figure the data are compared with the relevant curve, calculated according to the kinematics, and are found to be in very good agreement, supporting the accuracy of the data reconstruction. The beam charge was collected by a Faraday cup set at the entrance of MAGNEX, and its absolute value was cross-checked via the measurements at the most forward angles, where cross sections calculated with different optical potentials coincide, since they are close to Rutherford scattering. For extraction of the cross sections, counts were integrated over an angular step of ≈0.5°. The solid angle, defined by four slits located 250 mm downstream of the target, was calculated taking into account the contour of the reconstructed (θ_i, ϕ_i) locus [20] with an estimated uncertainty of ≈2%.

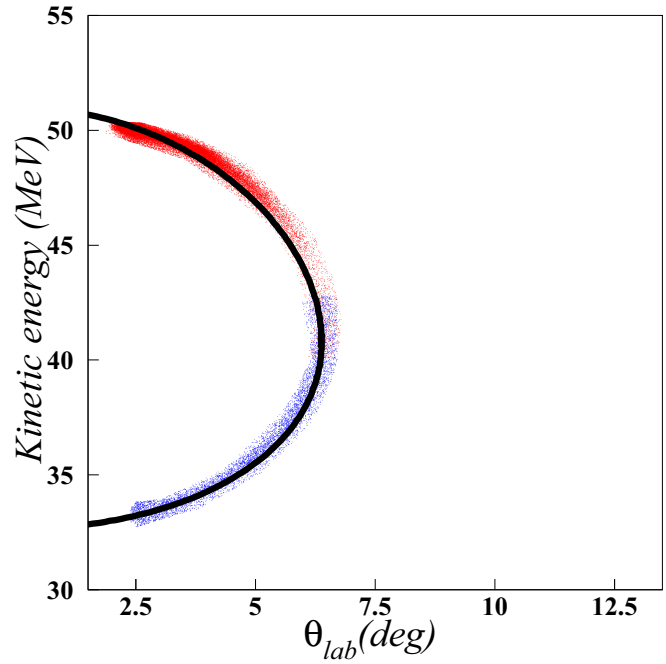

FIG. 1. Reconstructed E-θ correlation plot for $^{9}Be + p$ at a ^{9}Be projectile energy of 51 MeV. The two kinematical solutions of the reaction were obtained in two different runs with two sets of magnetic fields. The plot shows the superposition of these runs, designated by different colors. The solid black line represents the theoretical prediction which describes adequately the data, giving further support to the accuracy of the spectrum reconstruction.

III. EXISTING DATA SETS AND THEIR ABSOLUTE NORMALIZATIONS

As mentioned in Sec. I, the absolute normalizations of different existing data sets can differ by as much as 15% to 20%, where they overlap. This makes a consistent analysis of a combined set of data from various sources over a range of incident proton energies problematic, since if these discrepancies in absolute normalization are not addressed they can introduce spurious energy dependencies into the results of such an analysis. These considerations do not, of course, apply to analyzing power measurements since these are relative quantities.

We have already explained the rationale behind our choice of the data of Votava *et al.* as our benchmark. We now give details of the renormalizations necessary to produce a combined data set, consistent with this choice and the justifications. The 15 MeV elastic and inelastic scattering differential cross section data of Votava *et al.* [13] and Bingham *et al.* [15] match very well in shape, but the data of Bingham *et al.* require a renormalization factor of 0.85 in order to match the magnitude of the Votava *et al.* data. It should be noted, however, that this difference is within the stated uncertainties

TABLE I. Summary of renormalization factors applied in this work to data from the literature in order to achieve a consistent data set.

E_p (MeV)	Elastic scattering	Inelastic scattering	(p, d)
15	1.0 [13], 0.85 [15]	1.0 [13], 0.85 [15]	1.0 [14]
10	0.85 [15]	0.85 [15]	0.75 [24]
9	0.85 [15]	0.85 [15]	0.75 [24]
8	1.0 [21], 0.85 [15]	0.85 [15]	0.75 [24]
7	0.85 [15]	0.85 [15]	1.0 [25], 0.75 [24]
6	1.0 [22], 0.80 [15], 0.75 [21]	1.0 [22], 0.80 [15], 0.75 [21]	0.75 [24], 0.75 [21]
5	0.80 [15]	0.80 [15]	0.75 [24]
3	0.80 [23]		1.0 [32]

of the absolute normalizations of the two data sets. The same renormalization factor was applied to the elastic and inelastic scattering data of Bingham *et al.* [15] at 10, 9, 8, and 7 MeV. With this normalization the 8 MeV elastic scattering data of Bingham *et al.* also matched very well with the 8 MeV elastic scattering data of Blieden *et al.* [21].

At 6 MeV we renormalized the elastic and inelastic scattering data of Bingham *et al.* by a factor of 0.8 and Blieden *et al.* by a factor of 0.75 to match the the 6.1 MeV data of Ishiwari [22]. This may appear inconsistent with the previous factors; however, at least for the data set of Bingham *et al.* it is stated that "At the lower energies a 0.45 mg/cm^2 foil was used. Thicker targets were used at some of the higher energies where particle energy loss effects were not so important." so the slight difference in normalization could be due to the uncertainties in the thicknesses of the different targets. We therefore also used the 0.8 renormalization factor for the 5 MeV data of Bingham *et al.*. The renormalization factor of 0.8 MeV was also applied to the 3 MeV elastic scattering data of Loyd and Haeberli [23] since these data were effectively normalized to those of Bingham *et al.*.

The 7 MeV (p, d) data of Hudson *et al.* [24] were renormalized by a factor of 0.75 to match the data of Yanuba *et al.* [25] at the same energy. This factor was uniformly applied to the (p, d) data of Hudson *et al.* at all other energies. The 6 MeV (p, d) data of Blieden *et al.*, when renormalized by the same factor of 0.75 applied to their elastic and inelastic scattering data at this energy, matched well the renormalized data of Hudson *et al.* at the same energy. We summarize the various normalizations in Table I for convenience.

IV. COUPLED REACTION CHANNELS CALCULATIONS

As described in the previous section, we took the 15 MeV $p + {}^9$Be elastic and inelastic (to the 2.43 MeV $5/2^-$ resonance) scattering measurement of Votava *et al.* [13] as our benchmark since a rather complete set of data for the channels of interest exists at this proton energy; in addition to the scattering data, which include analyzing power measurements, there are also data for the ${}^9\text{Be}(p, d){}^8\text{Be}$ reaction leading to both the 0 MeV 0^+ and 3.03 MeV 2^+ resonances of ^{8}Be from a separate source [14].

The ensemble of data at 15 MeV were analyzed via coupled-reaction-channels (CRC) calculations employing the coupling scheme shown schematically in Fig. 2. All calculations were performed with the code FRESCO [26] or its searching version, SFRESCO. The $\langle d \mid p + n \rangle$ overlap was calculated using the Reid soft core potential [27] and included the small D-state component while the $\langle {}^9\text{Be} \mid {}^8\text{Be} + n \rangle$ overlaps used the spectroscopic factors of Cohen and Kurath [28]. The transferred neutron was bound in a Woods-Saxon well of radius $1.25 \times 8^{1/3}$ fm and diffuseness 0.65 fm with a spin-orbit term of Thomas form and a fixed depth of 6 MeV. The depth of the central well was adjusted to reproduce the experimental binding energy.

The coupling between the two ^{8}Be resonances in the exit partition assumed the standard rotational model, with the intrinsic matrix element $Mn(E2)$ obtained from the intrinsic quadrupole moment Q_0 given by Maris *et al.* [29] assuming a $K = 0$ band, and with the nuclear deformation length δ_2 derived from $Mn(E2)$ via the usual collective model expression and assuming a charge radius of $1.3 \times 8^{1/3}$ fm. The $d + {}^8$Be optical model potential was fixed in the following fashion. The $d + {}^8$Be elastic scattering at the appropriate energy was first calculated using the global deuteron optical parameters for $1p$-shell nuclei of Zhang *et al.* [30]. The resulting angular distribution was then fitted by a coupled channel (CC) calculation including the ${}^8\text{Be}\ 0^+ \rightarrow 2^+$ coupling, the potential parameters being adjusted using SFRESCO. The values are given in Table II.

The entrance channel coupling again assumed the rotational model, the three ^{9}Be states being considered to form a $K = 3/2$ rotational band. The $Mn(E2)$ was derived from the measured ground state spectroscopic quadrupole moment Q_s [31] and the nuclear deformation length δ_2 was adjusted to give the best description of the data for inelastic scattering to the 2.43 MeV $5/2^-$ state [13], resulting in a value of 2.45 fm. The initial entrance channel optical potential parameters were taken from Table 2 of Votava *et al.* [13] and were searched using SFRESCO to obtain the best fit to the elastic scattering

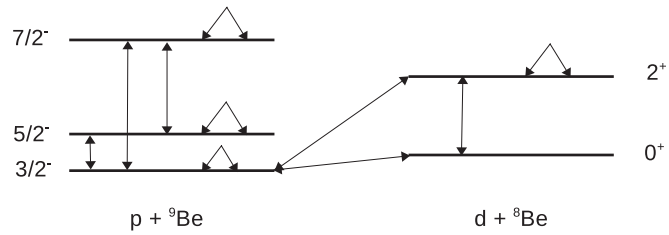

FIG. 2. Schematic of the coupling scheme used in the CRC calculations.

TABLE II. Optical potential parameters obtained by fitting $d + {}^{8}$Be elastic scattering angular distributions calculated using the global optical potential of Ref. [30] with CC calculations. The energies given are for the incident protons in the ${}^{9}\mathrm{Be}(p, d){}^{8}$Be reaction. Radii follow the convention $R_i = r_i \mathrm{A_t}^{1/3}$ fm and $r_\mathrm{C} = 1.3$ fm.

E_p (MeV)	V	r_V	a_V	W	r_W	a_W	W_d	r_d	a_d
15	141.1	1.035	0.776	4.26	2.062	0.744	3.52	2.062	0.744
10	61.7	1.035	0.468	1.13	1.308	0.744	3.93	2.493	0.712
9	130.2	1.032	0.802	4.42	1.243	0.744	5.17	2.076	0.853
8	67.7	0.969	0.862				4.64	2.174	0.875
7	67.3	0.983	0.793				4.16	2.219	0.862
6	210.0	1.063	0.685	8.84	1.625	0.506	2.52	2.463	0.850
5.70	201.0	1.025	0.776	10.2	1.273	0.654	4.31	2.289	0.838
5	129.5	1.009	0.822	7.05	1.976	0.601	2.45	2.443	0.741
3	199.1	1.027	0.836	5.87	2.079	0.744	5.86	1.887	0.728

data by CRC calculations using the full coupling scheme of Fig. 2. The resulting values are given in Table III.

In Fig. 3 we compare the results of the best-fit calculation with the data. The agreement with the elastic scattering is similar to that obtained by the CC calculations of Votava *et al.* [13] with the exception of the analyzing power for angles $\theta_\mathrm{c.m.} > 120^\circ$. The inelastic scattering data are not well described; the calculation is unable to reproduce the shape of the angular distributions and in this respect is similar to the CC calculations of Votava *et al.* [13]. The value of δ_2 chosen is something of a compromise since it would require an unphysically large value of this parameter to match the magnitude of the measured inelastic scattering cross section at angles $\theta_\mathrm{c.m.} < 90^\circ$. The (p, d) pickup data to both ^{8}Be states are reasonably well described, given that the exit channel optical potential was of necessity based on a global parameter set.

Similar CRC calculations were compared with the data for successively lower incident proton energies. All inputs were held fixed at the values used for $E_p = 15$ MeV with the exception of the exit channel deuteron optical potential parameters. These were derived in the same manner as at 15 MeV for the appropriate deuteron energies. The resulting parameters are given in Table II. We emphasize that this is the only energy dependence introduced into the inputs to the CRC calculations, all others being held fixed. Note that for incident proton energies below 3 MeV the global deuteron optical potential parameters of Ref. [30] were used unaltered since at these energies pickup to the 3.03 MeV 2^+ state is a closed channel and the ${}^{8}\mathrm{Be}\ 0^+ \rightarrow 2^+$ coupling was therefore dropped from the coupling scheme. Coupling to the 6.38 MeV $7/2^-$ state of ^{9}Be was dropped for incident proton energies $E_p \leqslant 7$ MeV and to the 2.43 MeV $5/2^-$ state for $E_p \leqslant$ 2.46 MeV for the same reason (ground state reorientation of ^{9}Be was retained at all energies).

TABLE III. Optical potential parameters obtained by fitting the 15 MeV $p + {}^{9}$Be elastic scattering data of Ref. [13] with a CRC calculation using the full coupling scheme of Fig. 2. Radii follow the convention $R_i = r_i \mathrm{A_t}^{1/3}$ fm and $r_\mathrm{C} = 1.33$ fm.

V	r_V	a_V	W_d	r_d	a_d	V_{so}	r_{so}	a_{so}
48.4	1.26	0.489	7.0	1.604	0.373	5.0	1.35	0.33

At $E_p = 10$ MeV, see Figs. 4(a)–4(d), not only is the angular distribution of the elastic scattering differential cross section of Bingham *et al.* [15] (after application of the renormalization factor of 0.85) well described over the whole angular range but also the elastic scattering analyzing power of Loyd and Haeberli [23]. The differential cross section for

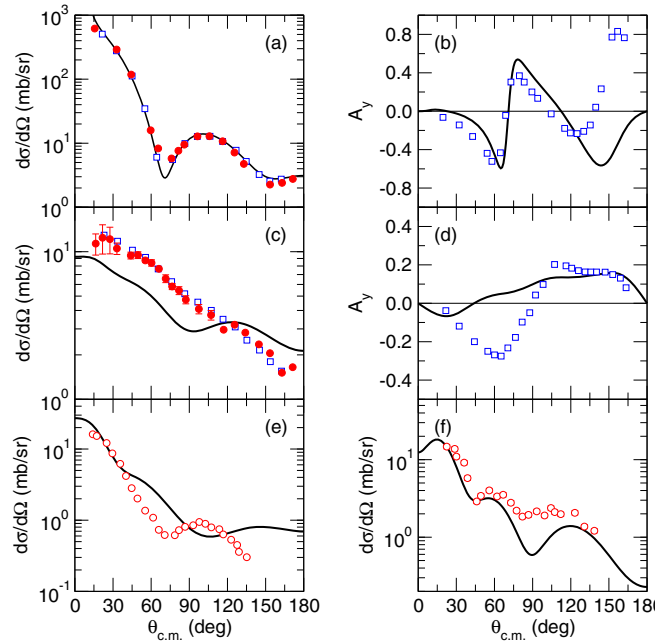

FIG. 3. (a) Elastic scattering differential cross section and (b) analyzing power angular distributions for 15 MeV protons incident on ^{9}Be. The open blue squares denote the data of Ref. [13] and the filled red circles the data of Ref. [15] renormalized by a factor of 0.85. The full curves denote the result of the CRC calculation described in the text. (c) and (d) As for (a) and (b) but for the inelastic scattering to the 2.43 MeV $5/2^-$ state of ^{9}Be. Angular distributions of the differential cross section for the ${}^{9}\mathrm{Be}(p, d){}^{8}$Be reaction leading to (e) the 0.0 MeV 0^+ and (f) the 3.03 MeV 2^+ states of ^{8}Be. The open red circles denote the data of Ref. [14] and the solid curves the result of the CRC calculation described in the text.

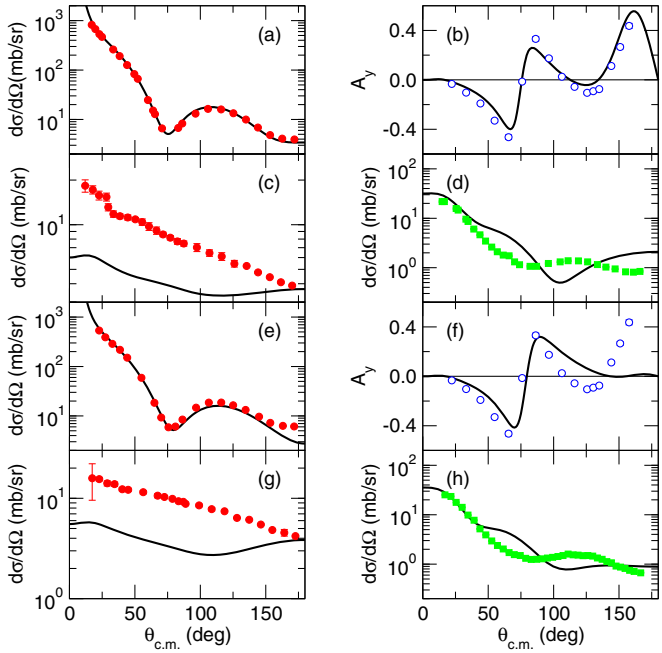

FIG. 4. (a) Elastic scattering differential cross section and (b) analyzing power angular distributions for 10 MeV protons incident on ^{9}Be. (c) Angular distribution for inelastic scattering to the 2.43 MeV $5/2^{-}$ state of ^{9}Be and (d) for the $^{9}\mathrm{Be}(p,d)^{8}\mathrm{Be}$ reaction leading to the 0.0 MeV 0^{+} state of ^{8}Be for 10 MeV protons incident on ^{9}Be. (e)–(h) As for (a)–(d) but for 9 MeV protons. The filled red circles denote the data of Ref. [15], renormalized by a factor of 0.85, the open blue circles the data of Ref. [23], and the filled green squares the data of Ref. [24], renormalized by a factor of 0.75. The full curves denote the results of the CRC calculations described in the text.

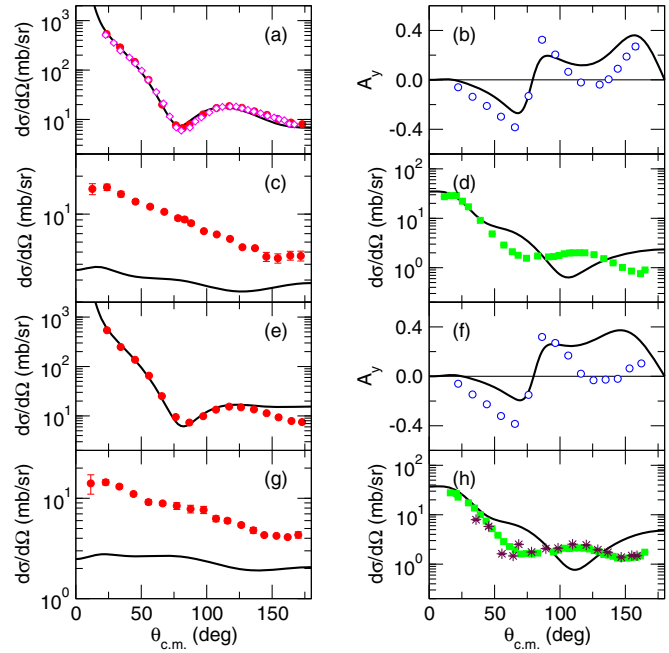

FIG. 5. (a) Elastic scattering differential cross section and (b) analyzing power angular distributions for 8 MeV protons incident on ^{9}Be. (c) Angular distribution for inelastic scattering to the 2.43 MeV $5/2^{-}$ state of ^{9}Be and (d) for the $^{9}\mathrm{Be}(p,d)^{8}\mathrm{Be}$ reaction leading to the 0.0 MeV 0^{+} state of ^{8}Be for 8 MeV protons incident on ^{9}Be. (e)–(h) As for (a)–(d) but for 7 MeV protons. The filled red circles denote the data of Ref. [15], renormalized by a factor of 0.85, the open blue circles the data of Ref. [23], and the filled green squares the data of Ref. [24], renormalized by a factor of 0.75. The open magenta diamonds denote the 8 MeV elastic scattering data of Blieden *et al.* [21] while the maroon stars denote the 7 MeV (p,d) data of Yanuba *et al.* [25]. The full curves denote the results of the CRC calculations described in the text.

inelastic scattering to the 2.43 MeV $5/2^{-}$ state is poorly described, as at $E_p = 15$ MeV the calculations fail to reproduce both the shape and magnitude of the data of Bingham *et al.* [15] (again renormalized by a factor of 0.85). The (p,d) pickup data to the 0.0 MeV 0^{+} state of ^{8}Be of Hudson *et al.* [24] (with the renormalization factor of 0.75) are reasonably well described, the forward angle data being slightly over predicted. The description of the data at $E_p = 9$ MeV is similar [see Figs. 4(e)–4(h)], the elastic scattering being less well described at large angles while the description of the forward angle pickup data is better, the magnitude being well reproduced. At $E_p = 8$ and 7 MeV (see Fig. 5) the description of the data remains comparable to that at the higher energies although the elastic scattering analyzing power is not as well reproduced and a noticeable deviation of the calculated from the measured elastic scattering cross section at backward angles is apparent at $E_p = 7$ MeV.

Further reduction in E_p to 6 and 5 MeV leads to a significant deterioration in the description of the elastic scattering angular distributions, both of the differential cross section and the analyzing power; see Fig. 6. The differential cross section is now only reproduced for angles up to the interference minimum at $\theta_{\mathrm{c.m.}} \approx 85^{\circ}$. However, relatively small adjustments to the depths of the real and imaginary parts of the entrance channel optical potential will recover a good description of the elastic scattering at these energies.

This trend continues as the incident proton energy is reduced to 3 MeV; see Fig. 7. The elastic scattering cross section is now only described at the most forward angles, the calculation considerably underpredicting the data for the rest of the angular range. However, the $^{9}\mathrm{Be}(p,d)^{8}\mathrm{Be}$ data remain as well described as at the higher incident energies. This energy is in the region of ^{10}B resonances in the $p + {}^{9}$Be elastic scattering and is also sufficiently low that significant compound nucleus contributions may be present in the remaining open channels. It is therefore not surprising that a CRC calculation based on an optical potential fixed at a considerably higher incident energy is unable to provide a good description of the elastic scattering over the whole angular range, although it is encouraging that the forward angles are well described, exactly where any compound nucleus and/or resonance effects should be small. The relatively good description of the (p,d) data—comparable to those at the higher incident energies—suggests that this particular reaction is still dominated at least at forward angles by the direct reaction component.

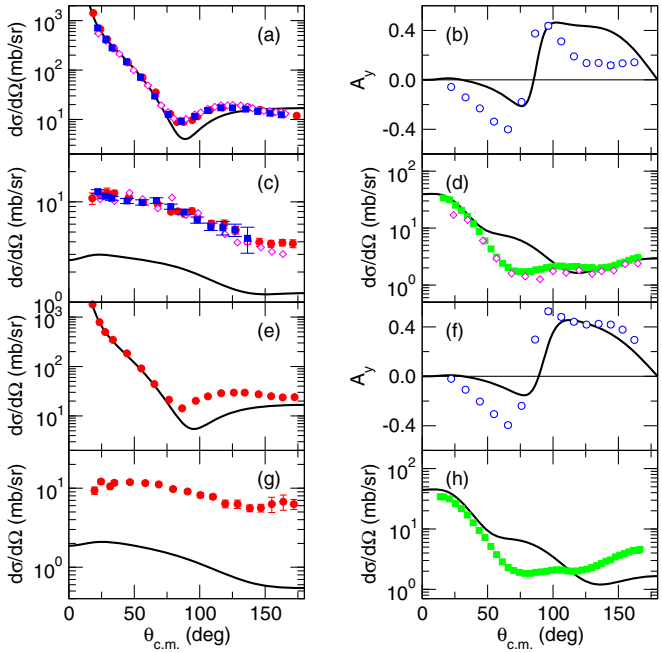

FIG. 6. (a) Elastic scattering differential cross section and (b) analyzing power angular distributions for 6 MeV protons incident on ^{9}Be. (c) Angular distribution for inelastic scattering to the 2.43 MeV $5/2^{-}$ state of ^{9}Be and (d) for the ^{9}Be$(p,d)^{8}$Be reaction leading to the 0.0 MeV 0^{+} state of ^{8}Be for 6 MeV protons incident on ^{9}Be. (e)–(h) As for (a)–(d) but for 5 MeV protons. The filled red circles denote the data of Ref. [15], renormalized by a factor of 0.8, the open blue circles the data of Ref. [23], and the filled green squares the data of Ref. [24], renormalized by a factor of 0.75. The open magenta diamonds denote the 6 MeV data of Blieden *et al.* [21] renormalized by a factor of 0.75 while the filled blue squares denote the 6.1 MeV data of Ishiwari [22]. The full curves denote the results of the CRC calculations described in the text.

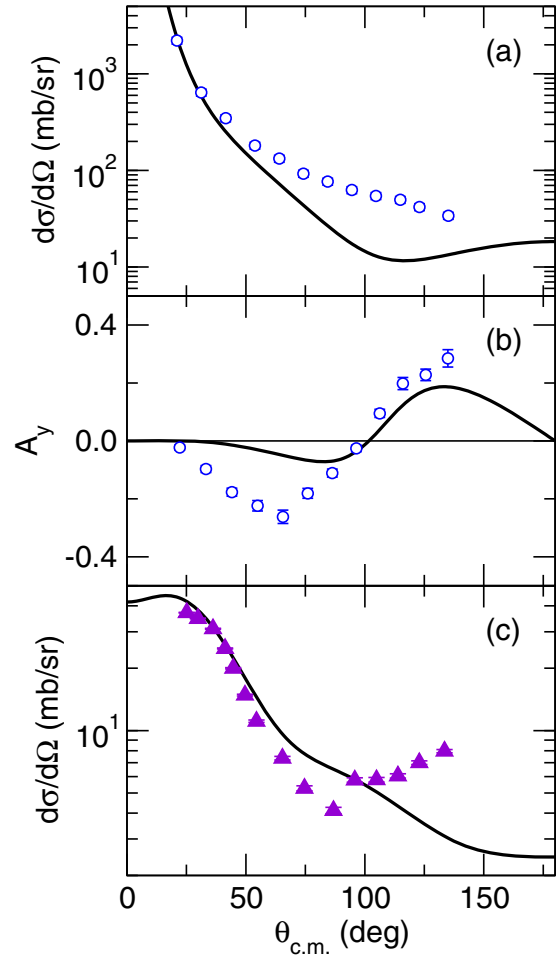

FIG. 7. Angular distributions for 3 MeV protons incident on ^{9}Be for (a) the elastic scattering differential cross section, (b) the elastic scattering analyzing power, and (c) the differential cross section for the ^{9}Be$(p,d)^{8}$Be reaction leading to the 0.0 MeV 0^{+} state of ^{8}Be. The open blue circles denote the data of Ref. [23], renormalized by a factor of 0.8 for the cross section, while the violet triangles denote the data of Morita *et al.* [32]. The full curves denote the results of the CRC calculations described in the text.

Finally, in Fig. 8 we compare the CRC calculations with the present elastic scattering data for equivalent incident proton energies of 5.70, 2.46 and 1.68 MeV. The angular distributions fit well into the trend of the existing data, with the exception of that at $E_p = 2.46$ MeV which shows a distinct minimum at $\theta_{\mathrm{c.m.}} \approx 100^{\circ}$ not apparent in either the existing data at 3 MeV [23] or the present data at 1.68 MeV. The CRC calculation slightly overpredicts the 5.70 MeV data at forward angles but in all other respects the description is comparable with that of the existing data at 5 and 6 MeV. The 2.46 MeV data are reasonably well described up to the minimum, again with a slight overprediction, while at 1.68 MeV the calculation significantly overpredicts the data except for the most forward measured angle. The (p,d) data of Ref. [32] at $E_p = 2.56$ MeV are also well described by the 2.46 MeV CRC calculations, the agreement being comparable to that shown in Fig. 7(c) for the 3 MeV data.

V. DISCUSSION

In the previous section we compared both the present data and data taken from the literature for the $p + {}^{9}$Be system with a set of CRC calculations where, apart from the omission of channels as they became classically closed, only the exit channel deuteron optical potential varied with incident proton energy. Given our assumption of the data of Votava *et al.* [13] as benchmark and the concomitant renormalization factors for some of the other data sets available in the literature, we obtained a consistent picture over the range of incident proton energies from 1.68 to 15 MeV.

The agreement of the CRC calculations with the elastic scattering differential cross sections may be qualified as "good" for incident energies down to 7 MeV and "reasonable" for energies down to about 5 MeV, although this is of course a subjective judgment. Relatively small adjustments in the depths of the real and imaginary parts of the entrance channel optical potential can give good fits to the data over the whole energy range at the price of introducing some energy dependence of the parameters for $E_p \leqslant 7$ MeV. For incident energies below 5 MeV we enter the region of ^{10}B resonances and possible compound nucleus contributions. The work of Krat *et al.* [33] compiles existing and new measurements of the

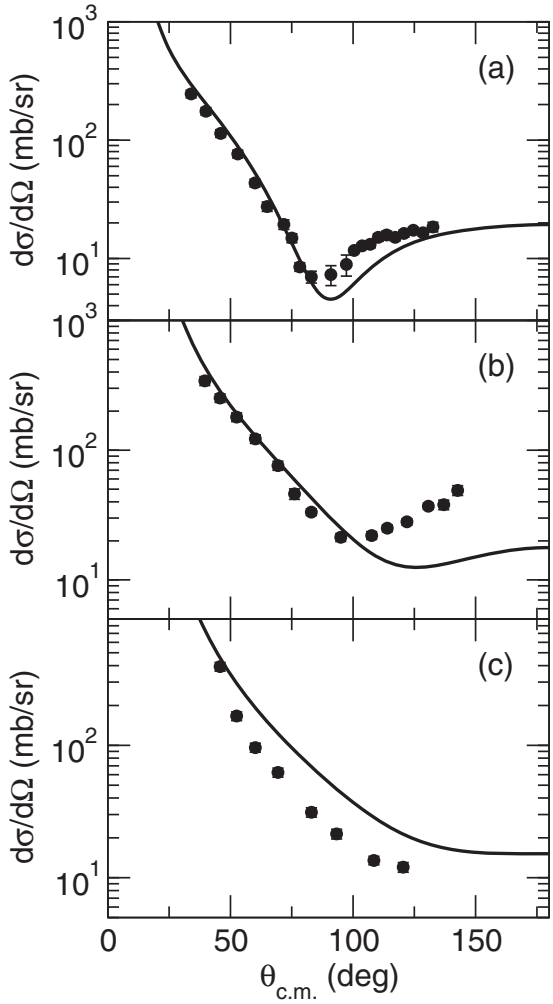

FIG. 8. Present data denoted by the filled black circles: Angular distributions of the ^{9}Be + p elastic scattering differential cross in inverse kinematics at equivalent incident proton energies of (a) 5.70 MeV, (b) 2.46 MeV, and (c) 1.68 MeV. The full curves denote the results of the CRC calculations described in the text.

backward-angle differential cross sections for the ^{9}Be(p, p_0), (p, d_0), and (p, α_0) reactions over the incident energy range from 0.4 to 4.15 MeV. From their Fig. 5 it is seen that the 3 MeV data of Ref. [23] are clear of any resonant behavior at backward angles while the present 2.46 MeV data match almost exactly in energy a pronounced resonant peak, thus explaining the apparent anomalous behavior of the measured elastic scattering angular distribution at this energy; the rise in cross section for angles $\theta_{\text{c.m.}} > 100^\circ$ are completely consistent with this. The 1.68 MeV data, however, again appear to be clear of any obvious resonant behavior, consistent with the measured angular distribution.

The above considerations suggest that the progressively worse description of the elastic scattering data as the incident energy is reduced could be largely due to missing reaction couplings, although some compound elastic contribution cannot be ruled out, except at 1.68 MeV where the data are overpredicted by the CRC calculations (since compound elastic contributions add incoherently to the direct scattering they cannot reduce the calculated cross section). At the lowest energies, apart from a very small amount of breakup (just above threshold), the only open channel not included in the calculations is the ^{9}Be$(p, \alpha_0)^6$Li reaction with a Q value of +2.13 MeV. The cross section has been measured in this energy regime and is significant [32]. However, test calculations (including the heavy particle pickup mode) were unable to reproduce the forward-angle data at $E_p = 3$ MeV, so that we are unable to confirm by explicit calculation whether coupling to this channel would improve the agreement with the elastic scattering data at the lowest energies.

The CRC calculations, however, completely fail to describe the data for inelastic scattering to the 2.43 MeV $5/2^-$ state. The shapes of the calculated angular distributions compared to the measured ones indicate that this discrepancy cannot be explained by a substantial compound contribution, so that the failure to describe these data must be more fundamental in nature. While the standard rotational model form factor appears to work well for ^{9}Be scattering from heavier targets (see, e.g., the analysis of ^{12}C(^{9}Be, ^{9}Be$'$) data of Rudchik *et al.* [34]), it fails completely to describe proton inelastic scattering. Test calculations confirmed that the omission of the small $\lambda = 4$ coupling within the ground state $K = 3/2$ rotational band, included in Ref. [34], did not significantly affect this result. Since protons may penetrate into the nuclear interior it would appear that proton scattering exposes the limitations of the standard collective rotational model form factor when applied to ^{9}Be, a nucleus which is known to exhibit pronounced clustering; and form factors calculated using a formalism that takes this into account, e.g., that of Ref. [35], will be required to fit the proton inelastic scattering.

On the other hand, the ^{9}Be$(p, d)^8$Be data are reasonably well described by the CRC calculations, especially given that global deuteron optical potential parameters must be used in the exit channel (albeit adapted to $1p$-shell target nuclei). This suggests that the reaction mechanism for this process is dominated by direct neutron stripping.

In summary, a coherent picture of the $p + ^9$Be scattering system emerges from our analysis, which the present measurements of the elastic scattering fit into in a consistent way. The absolute normalization of the present data appears to match well with our chosen benchmark, thus justifying its use to normalize the breakup coincidence data currently in the course of analysis. Our analysis also shows that the standard collective model form factor is inadequate to describe the inelastic scattering of protons from ^{9}Be, suggesting that a more realistic approach based on a picture that takes the pronounced clustering nature of ^{9}Be into account is necessary to describe these data. We see little evidence for a significant compound elastic contribution to the elastic scattering even at the lowest investigated energies.

ACKNOWLEDGMENTS

The research leading to these results has received funding from the European Union HORIZON2020 research and innovation program under Grant Agreement No. 654002-ENSAR2. One of us (L.A.) acknowledges partial support by CONACyT-LN294537 and PAPIIT-IA103218 Projects.

[1] V. Soukeras, A. Pakou, F. Cappuzzello *et al.*, Phys. Rev. C **91**, 057601 (2015).
[2] A. Pakou, V. Soukeras, F. Cappuzzello *et al.*, Phys. Rev. C **94**, 014604 (2016).
[3] A. Pakou, F. Cappuzzello, N. Keeley *et al.*, Phys. Rev. C **96**, 034615 (2017).
[4] Ch. Betsou, A. Pakou, F. Cappuzzello *et al.*, Eur. Phys. J. A **51**, 86 (2015).
[5] V. Soukeras, A. Pakou, F. Cappuzzello *et al.*, Phys. Rev. C **95**, 054614 (2017).
[6] A. Pakou, O. Sgouros, V. Soukeras, F. Cappuzzello *et al.*, Phys. Rev. C **95**, 044615 (2017).
[7] A. Pakou, N. Keeley, F. Cappuzzello *et al.*, Eur. Phys. J. A **53**, 167 (2017).
[8] S. E. Woosley and R. D. Hoffman, Astrophys. J. **395**, 202 (1992).
[9] B. S. Meyer, G. J. Mathews, W. M. Howard, S. E. Woosley, and R. D. Hoffman, Astrophys. J. **399**, 656 (1992).
[10] W. M. Howard, S. Goriely, M. Rayet, and M. Arnould, Astrophys. J. **417**, 713 (1993).
[11] S. E. Woosley, J. R. Wilson, G. J. Mathews, R. D. Hoffman, and B. S. Meyer, Astrophys. J. **433**, 229 (1994).
[12] W. von Oertzen, M. Freer, and Y. Kanada En'yo, Phys. Rep. **432**, 43 (2006).
[13] H. J. Votava, T. B. Clegg, E. J. Ludwig, and W. J. Thompson, Nucl. Phys. A **204**, 529 (1973).
[14] S. E. Darden, G. Murillo, and S. Sen, Nucl. Phys. A **266**, 29 (1976).
[15] F. W. Bingham, M. K. Brussel, and J. D. Steben, Nucl. Phys. **55**, 265 (1964).
[16] F. Cappuzzello, C. Agodi, D. Carbone, and M. Cavallaro, Eur. Phys. J. A **52**, 167 (2016).
[17] F. Cappuzzello, M. Cavallaro, A. Cunsolo *et al.*, Nucl. Instrum. Methods Phys. Res., Sect. A **621**, 419 (2010).
[18] F. Cappuzzello, D. Carbone, and M. Cavallaro, Nucl. Instrum. Methods Phys. Res., Sect. A **638**, 74 (2011).
[19] M. Cavallaro, F. Cappuzzello, D. Carbone *et al.*, Nucl. Instrum. Methods Phys. Res., Sect. A **648**, 46 (2011).
[20] M. Cavallaro, F. Cappuzzello, D. Carbone *et al.*, Nucl. Instrum. Methods Phys. Res., Sect. A **637**, 77 (2011).
[21] H. R. Blieden, G. M. Temmer, and K. L. Warsh, Nucl. Phys. **49**, 209 (1963).
[22] R. Ishiwari, Bull. Inst. Chem. Res. Kyoto Univ. **39**, 287 (1961).
[23] D. H. Loyd and W. Haeberli, Nucl. Phys. A **148**, 236 (1970).
[24] G. M. Hudson, G. B. Crinean, D. T. Kelly, and B. M. Spicer, Nucl. Phys. A **184**, 175 (1972).
[25] T. Yanabu, S. Yamashita, S. Kakigi, D.-Ca. Nguyen, K. Takimoto, Y. Yamada, and K. Ogino, J. Phys. Soc. Jpn. **9**, 1818 (1964).
[26] I. J. Thompson, Comput. Phys. Rep. **7**, 167 (1988).
[27] R. V. Reid jr., Ann. Phys. (N.Y.) **50**, 441 (1968).
[28] S. Cohen and D. Kurath, Nucl. Phys. A **101**, 1 (1967).
[29] P. Maris, M. A. Caprio, and J. P. Vary, Phys. Rev. C **91**, 014310 (2015).
[30] Y. Zhang, D. Y. Pang, and J. L. Lou, Phys. Rev. C **94**, 014619 (2016).
[31] D. R. Tilley, J. H. Kelley, J. L. Godwin, D. J. Millener, J. E. Purcell, C. G. Sheua, and H. R. Weller, Nucl. Phys. A **745**, 155 (2004).
[32] S. Morita, T. Tohei, T. Nakagawa, T. Hasegawa, H. Ueno, and H. Chu-Chung, Nucl. Phys. **66**, 17 (1965).
[33] S. Krat, M. Mayer, and C. Porosnicu, Nucl. Instrum. Methods Phys. Res., Sect. B **358**, 72 (2015).
[34] A. T. Rudchik, O. A. Momotyuk, V. A. Ziman, A. Budzanowski, A. Szczurek, I. Skwirczyńska, S. Kliczewski, and R. Siudak, Nucl. Phys. A **662**, 44 (2000).
[35] P. Descouvemont and N. Itagaki, Phys. Rev. C **97**, 014612 (2018).